

# On the dependence of QCD splitting functions on the choice of the evolution variable

---

**S. Jadach,<sup>a</sup> A. Kusina,<sup>b</sup> W. Płaczek,<sup>c</sup> M. Skrzypek<sup>a</sup>**

<sup>a</sup>*Institute of Nuclear Physics, Polish Academy of Sciences,  
ul. Radzikowskiego 152, 31-342 Kraków, Poland*

<sup>b</sup>*Laboratoire de Physique Subatomique et de Cosmologie  
53 Rue des Martyrs Grenoble, France*

<sup>c</sup>*Marian Smoluchowski Institute of Physics, Jagiellonian University,  
ul. Łojasiewicza 11, 30-348 Kraków, Poland*

**ABSTRACT:** We show that already at the NLO level the DGLAP evolution kernel  $P_{qq}$  starts to depend on the choice of the evolution variable. We give an explicit example of such a variable, namely the maximum of transverse momenta of emitted partons and we identify a class of evolution variables that leave the NLO  $P_{qq}$  kernel unchanged with respect to the known standard  $\overline{\text{MS}}$  results. The kernels are calculated using a modified Curci–Furmanski–Petronzio method which is based on a direct Feynman-graphs calculation.

**KEYWORDS:** Splitting Functions, DGLAP, NLO, Monte Carlo, evolution

---

## Contents

<b>1</b>	<b>Introduction</b>	<b>1</b>
<b>2</b>	<b>Diagram Vg</b>	<b>3</b>
2.1	Cut-off on $\max\{k_{1\perp}, k_{2\perp}\} < Q$	4
2.2	Cut-off on $k_{1\perp} + k_{2\perp} < Q$	6
2.3	Cut-off on $ \vec{k}_{1\perp} + \vec{k}_{2\perp}  \leq Q$	7
2.4	Cut-off on rapidity	8
2.5	General rule	8
<b>3</b>	<b>Diagram Vf</b>	<b>9</b>
<b>4</b>	<b>Virtual diagrams</b>	<b>10</b>
<b>5</b>	<b>Combined Vg+Vf real diagrams</b>	<b>10</b>
<b>6</b>	<b>Added real and virtual diagrams</b>	<b>11</b>
<b>7</b>	<b>Br (ladder) graph and counter term</b>	<b>11</b>
<b>8</b>	<b>Conclusions</b>	<b>12</b>
<b>A</b>	<b>Change of ladder graph with cut-off</b>	<b>13</b>

---

## 1 Introduction

The choice of the evolution variable in the QCD evolution of the partonic densities is one of the key issues in the construction of any Monte Carlo parton shower [1]. The most popular choices are related to virtuality, angle or transverse momentum of the emitted partons [2–4]. At the LO level, commonly used for the simulations, the splitting functions are identical for all variables. In this note we investigate whether it is the case also beyond the LO. To calculate the evolution kernels we use slightly modified methodology of the Curci-Furmanski-Petronzio classical paper [5]. It is based on the direct calculation of the contributing Feynman graphs in the axial gauge, cf. [6]. The graphs are extracted by means of the projection operators which close the fermionic or gluonic lines, put incoming partons on-shell and extract pole parts of the expressions. The distinct feature of this approach is the fact that the singularities are regularized by means of the dimensional regularization, except for the “spurious” ones which are regulated by the PV (principal value) prescription. To this end a dummy regulator  $\delta$  is introduced with the help of the replacement

$$\frac{1}{ln} \rightarrow \frac{ln}{(ln)^2 + \delta^2(pn)^2}. \quad (1.1)$$

The regulator  $\delta$  is directly linked to the definition of the PV operation and has a simple geometrical cut-off-like interpretation. This way some of the poles in  $\epsilon$  are replaced by logarithms of  $\delta$ . For more

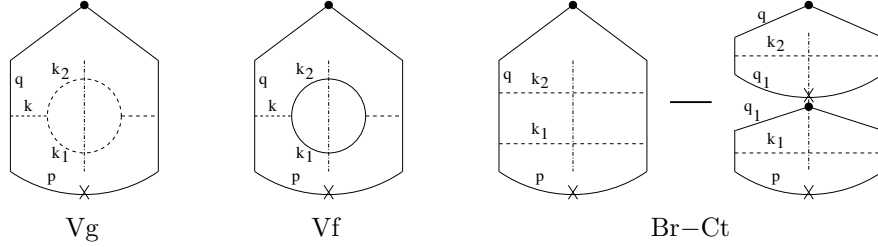


**Figure 1.** Real graphs with double poles contributing to the NLO non-singlet  $P_{qq}$  kernel.

details we refer to the original paper [5] or to later calculations, for example [7–9]. The difference of our method with respect to the approach of [5] is the use of the New PV (NPV) prescription which we have introduced in [10, 11]. It amounts to the extension of the geometrical regularization to all singularities in the light cone  $l^+$  variable, not only to the “spurious” ones. This modification turns out to be essential, as it further reduces the number of higher-order poles in  $\epsilon$  by replacing them with the  $\log \delta$  terms, and simplifies the contributions of individual graphs.

There are three mechanisms of keeping the kernel invariant under the change of the cut-off: (1) Invariance of a particular diagram. This applies to all diagrams with single poles in  $\epsilon$ . (2) Pairwise cancellation between matching real and virtual graphs, as in the Vg and Vf graphs of Fig. 1. (3) Cancellation between a graph and its counter-term. This is the case for ladder graphs. We will demonstrate that the mechanism (2) can fail already at the NLO level.

Our plan is the following. We will analyse the  $P_{qq}$  kernel. There are three graphs with second-order poles in  $\epsilon$  contributing to the kernel. They are depicted in Fig. 1. We will calculate the difference between the kernel with virtuality cut-off  $-q^2 < Q^2$ , as in the original paper [5], and with the set of different cut-offs. The cut-offs we consider are: the maximum and scalar sum of transverse momenta of the emitted partons, i.e.  $\max\{k_{1\perp}, k_{2\perp}\}$  and  $k_{1\perp} + k_{2\perp}$ , as well as the maximum and total rapidity of the emitted partons, i.e.  $\max\{k_{1\perp}/\alpha_1, k_{2\perp}/\alpha_2\}$  and  $|\vec{k}_{1\perp} + \vec{k}_{2\perp}|/(\alpha_1 + \alpha_2)$ .<sup>1</sup> The calculation will show that three of these cut-offs leave the kernel unchanged with respect to the known standard  $\overline{\text{MS}}$  results, whereas the one on the maximum of transverse momenta, changes the kernel. We will show in detail the mechanism of this change of the kernel and we will formulate a more general scheme of its analysis.

We will start from the diagram named Vg and its sibling Vf. Next we will discuss the ladder graph Br and its counter term, Ct. Our analysis will demonstrate that only the Vg and Vf diagrams depend on the chosen cut-off variable. In the case of the ladder graph the counter term cancels the dependence. Finally, we will comment why the graphs with only single  $\epsilon$  poles do not contribute. This is also the reason why NPV is instrumental: it replaces  $1/\epsilon^3$  poles of the diagram Yg (depicted in Fig. 2) by single poles and logarithms of the regulator  $\delta$ . As a consequence, this diagram does not contribute in NPV, whereas it would have a nontrivial contribution in the original PV prescription.

<sup>1</sup>We define  $k_{i\perp} \equiv |\vec{k}_{i\perp}|$ .

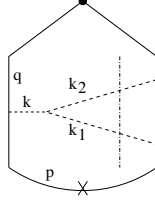


**Figure 2.** The graph Yg contributing to the NLO non-singlet  $P_{qq}$  kernel.

## 2 Diagram Vg

In order to establish our notation and conventions, we give explicitly the starting formula for the contribution of the diagram Vg, corresponding to Fig. 1:

$$\Gamma_G = c_G^V g^4 x \text{PP} \left[ \frac{1}{\mu^{4\epsilon}} \int d\Psi \delta\left(x - \frac{qn}{pn}\right) \frac{1}{q^4} W_G \right], \quad (2.1)$$

$$d\Psi = \frac{d^m k_1}{(2\pi)^m} 2\pi \delta^+(k_1^2) \frac{d^m k_2}{(2\pi)^m} 2\pi \delta^+(k_2^2) = (2\pi)^{-2m+2} \frac{1}{4} \frac{d\alpha_1}{\alpha_1} \frac{d\alpha_2}{\alpha_2} d^{m-2} \vec{k}_{1\perp} d^{m-2} \vec{k}_{2\perp}, \quad (2.2)$$

$$c_G^V = \frac{1}{2} C_G C_F, \quad (2.3)$$

$$W_G = \frac{1}{4qn} \frac{1}{k^4} \text{Tr} \left( \hat{n} \hat{q} \gamma^\mu \hat{p} \gamma^\lambda \hat{q} \right) d_{\nu''\nu'}(k_2) d_{\mu\mu''}(k_1 + k_2) d_{\lambda'\mu'}(k_1) d_{\mu'\lambda}(k_1 + k_2) \\ \times V(k_1^{\mu''} + k_2^{\mu''}, -k_2^{\nu''}, -k_1^{\lambda''}) V(k_1^{\mu'}, k_2^{\nu'}, -k_1^{\lambda'} - k_2^{\lambda'}). \quad (2.4)$$

We work in  $m = 4 + 2\epsilon$  dimensions. The Sudakov variables are defined with the help of the light-like vector  $n$  and the initial-quark momentum  $p$ :

$$k_i = \alpha_i p + \alpha_i^- n + k_{i\perp}^{(m)}, \quad q_i = x_i p + x_i^- n + q_{i\perp}^{(m)}, \quad (2.5)$$

$$p = (P, \vec{0}, P), \quad n = \left( \frac{pn}{2P}, \vec{0}, -\frac{pn}{2P} \right). \quad (2.6)$$

Note that the vector symbol  $\vec{\phantom{x}}$  denotes  $(m-2)$ -dimensional Euclidean vectors in transverse plane. Let us introduce new integration variables,  $\vec{\kappa}_1$  and  $\vec{\kappa}_2$ , instead of  $\vec{k}_{1\perp}$  and  $\vec{k}_{2\perp}$ :

$$\vec{k}_{1\perp} = \vec{\kappa}_1 - \vec{\kappa}_2, \quad \vec{k}_{2\perp} = \frac{\alpha_2}{\alpha_1} \vec{\kappa}_1 + \vec{\kappa}_2, \quad (2.7)$$

$$\text{i.e. } \vec{\kappa}_1 = \frac{\alpha_1}{\alpha_1 + \alpha_2} (\vec{k}_{1\perp} + \vec{k}_{2\perp}), \quad \vec{\kappa}_2 = \frac{\alpha_1 \alpha_2}{\alpha_1 + \alpha_2} \left( \frac{\vec{k}_{2\perp}}{\alpha_2} - \frac{\vec{k}_{1\perp}}{\alpha_1} \right), \quad (2.8)$$

$$\frac{\partial \vec{k}_{1\perp} \vec{k}_{2\perp}}{\partial \vec{\kappa}_1 \vec{\kappa}_2} = \left( \frac{1-x}{\alpha_1} \right)^{m-2}, \quad (2.9)$$

$$d\Psi = (2\pi)^{-2m+2} \frac{1}{4} \frac{d\alpha_1}{\alpha_1} \frac{d\alpha_2}{\alpha_2} \left( \frac{1-x}{\alpha_1} \right)^{m-2} \frac{1}{4} d\kappa_1^2 d\kappa_2^2 d\Omega_{m-3}^{(1)} d\Omega_{m-3}^{(2)} \kappa_1^{m-4} \kappa_2^{m-4}. \quad (2.10)$$

The benefit of these variables is the diagonal form of the variables  $k^2$  and  $q^2$  in which our formula is singular:

$$k^2 = \frac{(1-x)^2}{\alpha_1 \alpha_2} \kappa_2^2, \quad -q^2 = \frac{1-x}{\alpha_1} \left( \kappa_1^2 \frac{1}{\alpha_1} + \kappa_2^2 \frac{x}{\alpha_2} \right). \quad (2.11)$$

The trace  $W_G$  is of the form ( $\theta$  is the angle between  $\vec{\kappa}_1$  and  $\vec{\kappa}_2$ )

$$W_G = \frac{8}{x(1-x)^2} \left( \frac{\kappa_1^2}{\kappa_2^2} T_{Gc2} \cos^2 \theta + \sqrt{\frac{\kappa_1^2}{\kappa_2^2}} T_{Gc} \cos \theta + \frac{\kappa_1^2}{\kappa_2^2} T_{GK} + T_{Gn} \right), \quad (2.12)$$

$$T_{Gc2} = 4(1+\epsilon) \frac{x \alpha_2^2}{(1-x)^2}, \quad (2.13)$$

$$T_{Gc} = x(1+x) \left( (1+\epsilon) 2(\alpha_1 - \alpha_2) \frac{\alpha_2}{(1-x)^2} + \frac{\alpha_2 - \alpha_1}{\alpha_1} \right), \quad (2.14)$$

$$T_{GK} = \frac{\alpha_1^2 + \alpha_2^2}{\alpha_1^2} \left( 1 + x^2 + \epsilon(1-x)^2 \right) + \alpha_2^2(1+\epsilon), \quad (2.15)$$

$$T_{Gn} = (1+\epsilon) \frac{x^2}{(1-x)^2} (\alpha_1 - \alpha_2)^2. \quad (2.16)$$

This allows us to rewrite formula (2.1) as

$$\begin{aligned} \Gamma_G &= c_G^V g^4 x \text{PP} \left[ \frac{1}{\mu^{4\epsilon}} \int (2\pi)^{-2m+2} \frac{1}{4} \frac{d\alpha_1}{\alpha_1} \frac{d\alpha_2}{\alpha_2} \left( \frac{1-x}{\alpha_1} \right)^{m-2} \right. \\ &\quad \times \frac{1}{4} d\kappa_1^2 d\kappa_2^2 d\Omega_{m-3}^{(1)} d\Omega_{m-3}^{(2)} \kappa_1^{m-4} \kappa_2^{m-4} \delta_{1-x-\alpha_1-\alpha_2} \\ &\quad \left. \times \frac{1}{q^4} \frac{8}{x(1-x)^2} \left( \frac{\kappa_1^2}{\kappa_2^2} T_{Gc2} \cos^2 \theta + \sqrt{\frac{\kappa_1^2}{\kappa_2^2}} T_{Gc} \cos \theta + \frac{\kappa_1^2}{\kappa_2^2} T_{GK} + T_{Gn} \right) \right]. \end{aligned} \quad (2.17)$$

## 2.1 Cut-off on $\max\{k_{1\perp}, k_{2\perp}\} < Q$

Let us now perform the calculation of the Vg graph with the cut-off on the transverse momentum:  $\max\{k_{1\perp}, k_{2\perp}\} < Q$ . This diagram has two  $\epsilon$ -type singularities, related to  $1/q^2$  and  $1/\kappa_2^2 \sim 1/k^2$ . The kernel is constructed from the single-pole part of the diagram. Therefore, if we were able to separate the part of the diagram containing a double pole, we could considerably easier calculate the remaining single-pole part. This can be done if we calculate the difference between  $\max\{k_{1\perp}, k_{2\perp}\} < Q$  and the standard virtuality-based cut-off  $-q^2 < Q^2$ . This way we exclude the region of double pole. In the leftover difference the  $d\kappa_2^2$  integral has to generate pole in  $\epsilon$  and we can discard all terms finite in  $\epsilon$ .

We will compute

$$\Delta \Gamma_{Vg}^{k_{\perp} - q} = \Gamma_G (\max\{k_{1\perp}, k_{2\perp}\} < Q) - \Gamma_G (-q^2 < Q^2). \quad (2.18)$$

The  $-q^2 > Q^2$  translates into (see eq. (2.11))

$$-q^2 = c_1^2 \kappa_1^2 + c_2^2 \kappa_2^2 > Q^2 \Rightarrow \int_0^{\infty} d\kappa_2^2 (\kappa_2^2)^{-1+\epsilon} \int_{(1/c_1)^2 Q^2 - (c_2/c_1)^2 \kappa_2^2}^{\infty} d\kappa_1^2 \frac{(\kappa_1^2)^{1+\epsilon}}{(c_1^2 \kappa_1^2 + c_2^2 \kappa_2^2)^2}, \quad (2.19)$$

$$c_1^2 = \frac{1-x}{\alpha_1^2}, \quad c_2^2 = \frac{(1-x)x}{\alpha_1 \alpha_2}. \quad (2.20)$$

In eq. (2.19) we have shown only the singular parts of the integrand. The singularities of the integral are located at  $k^2 = \frac{(1-x)^2}{\alpha_1 \alpha_2} \kappa_2^2 = 0$ , i.e. at  $\kappa_2 = 0$  and at  $-q^2 = c_1^2 \kappa_1^2 + c_2^2 \kappa_2^2 = 0$  i.e. at  $\kappa_1 = \kappa_2 = 0$ . As we can see from (2.19), the  $q^2 = 0$  area is excluded due to subtraction of the  $\Gamma_G(-q^2 < Q^2)$  which is available in the literature [5, 8]. The external integrals over  $d\alpha$  cannot contribute additional  $1/\epsilon$  poles as they are regulated by the NPV prescription. This is one of the two key ingredients of the calculation. Since we are interested in the pole part of  $\Delta\Gamma$ , we can expand the  $d\kappa_2$  integrand in a standard way:

$$d\kappa_2^2 (\kappa_2^2)^{-1+\epsilon} = d\kappa_2^2 \frac{1}{\epsilon} \delta_{\kappa_2^2=0} + \mathcal{O}(\epsilon^0). \quad (2.21)$$

This allows us to set  $\kappa_2$  to zero in the rest of the formula (2.17), both in the integrand and in the integration limits. Furthermore, we can drop the terms  $T_{Gc}$  and  $T_{Gn}$  which do not have singularities in  $\kappa_2^2$ . Finally, we can set  $\epsilon$  to zero in the remaining part of the formula. Altogether we obtain

$$\begin{aligned} \Delta\Gamma_{Vg}^{k_\perp -q} &= c_G^V g^4 x (2\pi)^{-6} \frac{1}{2} \frac{1}{\epsilon} \frac{1}{x} \text{PP} \left[ \int \frac{d\alpha_1}{\alpha_1^3} \frac{d\alpha_2}{\alpha_2} \frac{1}{c_1^4} \delta_{1-x-\alpha_1-\alpha_2} \right. \\ &\quad \times \left. \int_{(1/c_1)^2 Q^2} \frac{d\kappa_1^2}{\kappa_1^2} \int d\Omega_1^{(1)} d\Omega_1^{(2)} (T_{Gc2} \cos^2 \theta + T_{GK}) \right]. \end{aligned} \quad (2.22)$$

Next, we have to fix the upper limit of the  $d\kappa_1$  integral. We have

$$\begin{aligned} \max\{k_{1\perp}, k_{2\perp}\} &< Q \\ \Rightarrow \max \left\{ |\vec{\kappa}_1 - \vec{\kappa}_2|, \left| \frac{\alpha_2}{\alpha_1} \vec{\kappa}_1 + \vec{\kappa}_2 \right| \right\} &< Q \\ \Rightarrow |\vec{\kappa}_1 - \vec{\kappa}_2| < Q, \quad \left| \frac{\alpha_2}{\alpha_1} \vec{\kappa}_1 + \vec{\kappa}_2 \right| &< Q. \end{aligned} \quad (2.23)$$

We are interested in the limits for  $\kappa_1$  at the point  $\kappa_2 = 0$ . Immediately from eq. (2.23) we find

$$\kappa_1 < Q, \quad \frac{\alpha_2}{\alpha_1} \kappa_1 < Q. \quad (2.24)$$

We have to discuss the integration limits for both of the angular integrals as well. One of the angles is trivial and covers the entire range  $(0, 2\pi)$ , as the system has rotational symmetry. The other angle,  $\theta$ , between  $\vec{\kappa}_1$  and  $\vec{\kappa}_2$ , has a non-trivial integration range, which depends on kappas and alphas. However, there is a subspace where this angle is also unlimited. It is given by the conditions

$$\kappa_1 + \kappa_2 < Q, \quad \frac{\alpha_2}{\alpha_1} \kappa_1 + \kappa_2 < Q. \quad (2.25)$$

It just happens that in the limit  $\kappa_2 = 0$  eq. (2.25) coincides with the entire range of  $\kappa_1$ . This way we

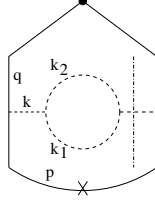


**Figure 3.** Real-virtual graph Vg contributing to NLO non-singlet  $P_{qq}$  kernel

find ( $c_0 = \alpha_2/\alpha_1$ )

$$\int_{(1/c_1)^2 Q^2}^{\min\{Q^2/c_0^2, Q^2\}} \frac{d\kappa_1^2}{\kappa_1^2} \int_0^{2\pi} d\Omega_1^{(1)} \int_0^{2\pi} d\theta (T_{Gc2} \cos^2 \theta + T_{GK}) \quad (2.26)$$

$$\begin{aligned} &= \left( \theta_{c_0 < 1} \ln c_1^2 + \theta_{c_0 > 1} \ln \frac{c_1^2}{c_0^2} \right) 2\pi (\pi T_{Gc2} + 2\pi T_{GK}) \\ &= \left( \theta_{\alpha_2 < \alpha_1} \ln \frac{1-x}{\alpha_1^2} + \theta_{\alpha_2 > \alpha_1} \ln \frac{1-x}{\alpha_2^2} \right) 4\pi^2 \frac{\alpha_2}{\alpha_1 x} T_S, \\ T_S &= x(1+x^2) \left( \frac{1}{(1-x)^2} \alpha_1 \alpha_2 + \frac{\alpha_1^2 + \alpha_2^2}{\alpha_1 \alpha_2} \right). \end{aligned} \quad (2.27)$$

Going back to eq. (2.22) we obtain

$$\Delta \Gamma_{Vg}^{k_\perp - q} = c_G^V \frac{g^4}{(2\pi)^4} \frac{1}{2\epsilon} \frac{1}{x(1-x)^2} \int d\alpha_1 d\alpha_2 \delta_{1-x-\alpha_1-\alpha_2} \left( \ln(1-x) - 4\theta_{\alpha_2 < \alpha_1} \ln \alpha_1 \right) T_S. \quad (2.28)$$

Performing the  $\alpha$ -integrals we find

$$\Delta \Gamma_{Vg}^{k_\perp - q} = c_G^V \left( \frac{\alpha_S}{\pi} \right)^2 \frac{1}{2\epsilon} \frac{1+x^2}{1-x} \left[ \ln \frac{1}{(1-x)} \left( 2I_0 + 2\ln(1-x) - \frac{11}{6} \right) - 4 \left( -\frac{11}{12} \ln 2 + \frac{131}{144} - \frac{\pi^2}{12} \right) \right] \quad (2.29)$$

where we have introduced the symbol  $I_0$  for the IR-divergent integral regularized by means of the PV prescription with the geometrical  $\delta$  parameter:

$$I_0 = \int_0^1 d\alpha \frac{\alpha}{\alpha^2 + \delta^2} = -\frac{1}{2} \ln \delta^2, \quad (2.30)$$

$$I_1 = \int_0^1 d\alpha \ln \alpha \frac{\alpha}{\alpha^2 + \delta^2} = -\frac{1}{8} \ln^2 \delta^2 - \frac{\pi^2}{24}. \quad (2.31)$$

The result (2.29) differs from the shift in virtual corrections that we show later in Section 4. We have obtained a net change of the kernel.

## 2.2 Cut-off on $k_{1\perp} + k_{2\perp} < Q$

We have demonstrated in the previous section that the change of real and virtual Vg-type diagrams do not compensate each other. Why is this so? Imagine the virtual correction Vg, Fig. 3. The graph has one real gluon, labelled  $k$ , and the cut-off is unique and trivial:  $k_\perp \leq Q$ . However, if we look inside the graph we find two virtual momenta,  $k_1$  and  $k_2$ , such that  $k_1 + k_2 = k$ . Therefore, our  $k_\perp$ -cut-off at the

unintegrated level is  $|\vec{k}_{1\perp} + \vec{k}_{2\perp}| \leq Q$ . This cut-off seems to be not good for real gluons because it does not close the phase space. We will come to this issue in the next paragraph. For now let us note that, as argued in Section 2.1, we calculate only the difference between the  $q^2$  and  $k_\perp$  cut-offs, and therefore we integrate only over the region singular in  $\kappa_2$ , i.e. we expand the  $d\kappa_2$  integral according to eq. (2.21). This introduces  $\kappa_2^2 = [\alpha_1\alpha_2/(1-x)^2]k^2 = 0$ , or equivalently  $\vec{k}_{1\perp}/\alpha_1 - \vec{k}_{2\perp}/\alpha_2 = 0$ . In this subspace the condition  $|\vec{k}_{1\perp} + \vec{k}_{2\perp}| \leq Q$  simplifies to  $\kappa_1^2 \leq [\alpha_1/(1-x)]^2 Q^2 = [1/(1+c_0)]^2 Q^2$ . In analogy, the “scalar” condition  $|\vec{k}_{1\perp}| + |\vec{k}_{2\perp}| \leq Q$  simplifies to  $|\vec{\kappa}_1| + |\vec{\kappa}_1|(\alpha_2/\alpha_1) \leq Q$ , i.e.  $\kappa_1^2 \leq [\alpha_1/(1-x)]^2 Q^2$ , identical to the previous cut-off. Therefore, we expect that the “scalar” cut-off  $|\vec{k}_{1\perp}| + |\vec{k}_{2\perp}| \leq Q$  will give the result compatible with the virtual correction. With this cut-off eq. (2.26) becomes

$$\begin{aligned} & \int_{(1/c_1)^2 Q^2}^{[1/(1+c_0)]^2 Q^2} \frac{d\kappa_1^2}{\kappa_1^2} \int_0^{2\pi} d\Omega_1^{(1)} \int_0^{2\pi} d\theta (T_{Gc2} \cos^2 \theta + T_{GK}) \\ &= \ln \frac{c_1^2}{(1+c_0)^2} 2\pi (\pi T_{Gc2} + 2\pi T_{GK}) \\ &= \ln \frac{1}{1-x} 4\pi^2 \frac{\alpha_2}{\alpha_1 x} T_S. \end{aligned} \quad (2.32)$$

Consequently, eq. (2.28) becomes

$$\Delta\Gamma_{Vg}^{\Sigma k_\perp - q} = c_G^V \frac{g^4}{(2\pi)^4} \frac{1}{2\epsilon} \frac{1}{x(1-x)^2} \int d\alpha_1 d\alpha_2 \delta_{1-x-\alpha_1-\alpha_2} \ln \frac{1}{1-x} T_S \quad (2.33)$$

$$= c_G^V \left( \frac{\alpha_S}{\pi} \right)^2 \frac{1}{2\epsilon} \frac{1+x^2}{1-x} \ln \frac{1}{1-x} \left( 2I_0 + 2\ln(1-x) - \frac{11}{6} \right). \quad (2.34)$$

This way we reproduced result (2.29), but without additional constant terms. It is identical to the change in virtual corrections and there is no modification of the kernel.

### 2.3 Cut-off on $|\vec{k}_{1\perp} + \vec{k}_{2\perp}| \leq Q$

Let us come back to the cut-off on vector variable  $|\vec{k}_{1\perp} + \vec{k}_{2\perp}| \leq Q$ . It indeed allows for arbitrarily big  $\vec{k}_{i\perp}$  vectors. The question is however whether it leads to well-defined and meaningful kernels? We will argue that it does.

Translated into  $\kappa$ -variables of eq. (2.8), the cut-off is simply  $\kappa_1 \leq \alpha_1/(1-x)Q$ , identical to the one of Section 2.2. The  $\vec{\kappa}_2 = \vec{\kappa}_1 - \vec{k}_{1\perp}$  variable is unbounded because so is  $\vec{k}_{1\perp}$  (the  $\vec{k}_{2\perp}$  can always be adjusted to fulfill the cut-off) and the angle is also unlimited,  $0 \leq \angle(\vec{\kappa}_1, \vec{\kappa}_2) \leq 2\pi$ . Keeping in mind the discussion on the origin of poles given around eq. (2.21), we conclude that the upper limit on  $\kappa_2$  does not matter at all, and we can set it to infinity as well. Repeating all the steps of Section 2.2 we recover the result (2.34). In other words, we have just shown that the cut-off  $|\vec{k}_{1\perp} + \vec{k}_{2\perp}| \leq Q$  leads to a proper kernel.

One may be worried about the higher order terms of  $\epsilon$ -expansion of eq. (2.21): are they finite? To answer this question let us inspect the original equations (2.1) and (2.12). In the limit  $\kappa_2^2 \rightarrow \infty$  we have  $-q^2 \sim (1-x)x/(\alpha_1\alpha_2)\kappa_2^2$  and we find integrals of the type

$$\int_0^\infty d\kappa_2^2 \left\{ \frac{1}{(\kappa_2^2)^3}, \frac{1}{(\kappa_2^2)^{5/2}}, \frac{1}{(\kappa_2^2)^2} \right\}, \quad (2.35)$$

which are integrable at the infinity. We conclude that the  $\epsilon$  expansion of eq. (2.21) is legitimate and the cut-off  $|\vec{k}_{1\perp} + \vec{k}_{2\perp}| \leq Q$  is self consistent. The open question is though how will this cut-off perform with other graphs. Another question concerns its generalization to more than two real partons.



## 2.4 Cut-off on rapidity

Let us briefly comment on the cut-off on rapidity. By rapidity we understand the quantity  $a = |\vec{k}_\perp|/\alpha$  (massless) or  $a = \sqrt{|\vec{k}_\perp|^2 + k^2}/\alpha$  (massive). For the case of two emissions the analogy to virtual graph leads to  $a = |\vec{k}_{1\perp} + \vec{k}_{2\perp}|/(\alpha_1 + \alpha_2) \leq Q$  or  $a = \sqrt{|\vec{k}_{1\perp} + \vec{k}_{2\perp}|^2 + (k_1 + k_2)^2}/(\alpha_1 + \alpha_2) \leq Q$ . In the subspace  $\kappa_2^2 \sim k^2 = 0$  both formulas coincide and both are identical to the  $k_\perp$ -type formula with the cut-off  $Q$  shifted to  $Q(1-x)$  in the  $k_\perp$ -type formula. This is just the result we have obtained for the virtual corrections. Another option is  $\max\{a_1, a_2\} \leq Q$ . We have  $\vec{a}_1 = (\vec{\kappa}_1 - \vec{\kappa}_2)/\alpha_1$  and  $\vec{a}_2 = \vec{\kappa}_1/\alpha_1 + \vec{\kappa}_2/\alpha_2$ . At  $\kappa_2 = 0$  this leads to  $\kappa_1/\alpha_1 \leq Q$  or equivalently  $|\vec{k}_{1\perp} + \vec{k}_{2\perp}|/(\alpha_1 + \alpha_2) \leq Q$ . This is identical to the previous case, so we expect the result to be in agreement with the virtual correction as well.

Let us compute the correction from the  $q^2$ -type to  $a$ -type cut-off. To this end we generalize eq. (2.26), which is the  $k_\perp$ -type, by replacing  $Q^2 \rightarrow Q^2(1-x)^\sigma$  in the upper limit:  $\sigma = 2$  corresponds to the rapidity case discussed here,  $\sigma = 0$  is the  $k_\perp$  case (reference) and  $\sigma = 1$  is the virtuality case (the correction vanishes). This is so because:  $\Sigma k_\perp = ((1-x)/\alpha_1)^2 \kappa_1^2 \leq Q^2$  is described by eq. (2.26).  $a = k_\perp/(1-x) \rightarrow \kappa_1/\alpha_1 \leq Q$  requires multiplication of  $Q^2$  by  $(1-x)^2$  (with respect to the  $k_\perp$  case).  $-q^2 \rightarrow (1-x)\kappa_1^2/\alpha_1^2 \leq Q^2$  requires multiplication of  $Q^2$  by  $1-x$ .

$$\begin{aligned} & \int_{(1/c_1)^2 Q^2}^{[(1-x)^\sigma/(1+c_0)]^2 Q^2} \frac{d\kappa_1^2}{\kappa_1^2} \int_0^{2\pi} d\Omega_1^{(1)} \int_0^{2\pi} d\theta (T_{Gc2} \cos^2 \theta + T_{GK}) \\ &= \ln \frac{c_1^2(1-x)^\sigma}{(1+c_0)^2} 2\pi (\pi T_{Gc2} + 2\pi T_{GK}) \\ &= \ln(1-x)^{\sigma-1} 4\pi^2 \frac{\alpha_2}{\alpha_1 x} T_S. \end{aligned} \quad (2.36)$$

Consequently, eq. (2.28) becomes

$$\begin{aligned} \Delta\Gamma_{Vg}^{\sigma-q} &= c_G^V \frac{g^4}{(2\pi)^4} \frac{1}{2\epsilon} \frac{1}{x(1-x)^2} \int d\alpha_1 d\alpha_2 \delta_{1-x-\alpha_1-\alpha_2} \ln(1-x)^{\sigma-1} T_S \\ &= c_G^V \left(\frac{\alpha_S}{\pi}\right)^2 \frac{1}{2\epsilon} \frac{1+x^2}{1-x} \ln(1-x)^{\sigma-1} \left(2I_0 + 2\ln(1-x) - \frac{11}{6}\right). \end{aligned} \quad (2.37)$$

## 2.5 General rule

We can now generalize the analysis of previous sections and formulate a more universal rule of identifying the variables that do or do not change the NLO kernel.

In Fig. 4 we show the  $(\kappa_1, \kappa_2)$  plane. The blue cut-off  $\vec{\kappa}_1 \leq Q$  is shown along with a family of other cut-off lines. Some of them (blue) are equivalent if they cross the  $\kappa_1$ -axis at the same point. The cut-offs may close the  $\kappa_2$ -direction from above or leave it open. At the bottom left we plot the red  $-q^2 \leq Q_0^2$  line. The singularities lie at the origin of the frame ( $q^2 = 0$ ) and along the line  $\kappa_2^2 \sim k^2 = 0$ . The integration path is the thick line along  $\kappa_2 = 0$  between crossing points of  $-q^2 = Q_0^2$  and the cut-off with the axis.

The strategy we use is the following. We take a group of variables that coincide at the LO level (i.e. for single emission), we express them in terms of the variables  $\kappa$  and we set  $\kappa_2 = 0$ . All the variables that cross the  $\kappa_1$  axis at the same point will lead to the same result. It is now a matter of choosing one of them, calculating the shift, as outlined in the paper, and comparing it with the shift in the virtual corrections. We collect the shifts in the virtual corrections for the basic three types of variables in Section 4.

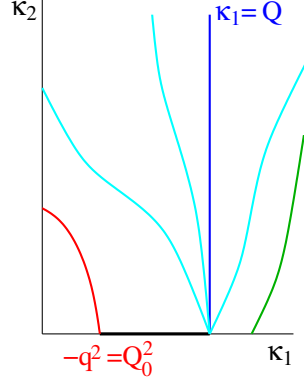


**Figure 4.** The  $(\kappa_1, \kappa_2)$  plane. The cut-off  $\kappa_1 \leq Q$  is shown in dark blue. A family of other cut-off lines is shown in light blue. At the bottom left the  $-q^2 \leq Q_0^2$  line is plotted in red. The singularities lie at the origin of the frame ( $q^2 = 0$ ) and along the line  $\kappa_2^2 \sim k^2 = 0$ . The integration path is the thick black line along  $\kappa_2 = 0$  between the crossing points of  $-q^2 = Q_0^2$  and the cut-off with the axis.

### 3 Diagram Vf

Let us now perform the analysis of the Vf graph. It will heavily rely on the analysis done for the Vg graph. Let us begin with the  $\max\{k_{1\perp}, k_{2\perp}\}$  calculation. Our starting point is the diagram depicted in Fig. 1. The analytical formula is analogous to eq. (2.1):

$$\Gamma_F = c_F^V g^4 x \text{PP} \left[ \frac{1}{\mu^{4\epsilon}} \int d\Psi \delta\left(x - \frac{qn}{pn}\right) \frac{1}{q^4} W_F \right], \quad (3.1)$$

$$c_F^V = C_F T_F, \quad (3.2)$$

$$\begin{aligned} W_F &= \frac{1}{4qn} \frac{1}{k^4} \text{Tr}(\hat{n} \hat{q} \gamma^\mu \hat{p} \gamma^\lambda \hat{q}) d_{\mu\mu''}(k_1 + k_2) \text{Tr}(\hat{k}_2 \gamma^{\mu''} \hat{k}_1 \gamma^{\mu'}) d_{\mu'\lambda}(k_1 + k_2) \\ &= \frac{32pn}{4qn} \frac{1}{(1-x)^2} \left( \frac{\kappa_1^2}{\kappa_2^2} T_{Fc2} \cos^2 \theta + \sqrt{\frac{\kappa_1^2}{\kappa_2^2}} T_{Fc} \cos \theta + \frac{\kappa_1^2}{\kappa_2^2} T_{FK} + T_{Fn} \right), \end{aligned} \quad (3.3)$$

$$T_{Fc2} = -4x \frac{\alpha_2^2}{v^2}, \quad (3.4)$$

$$T_{Fc} = 2x(1+x)\alpha_2(\alpha_2 - \alpha_1) \frac{1}{v^2}, \quad (3.5)$$

$$T_{FK} = \frac{1}{2} \epsilon v^2 \frac{\alpha_2}{\alpha_1} + \frac{1}{2} (1+x^2) \frac{\alpha_2}{\alpha_1} - \alpha_2^2, \quad (3.6)$$

$$T_{Fn} = 4 \frac{x^2}{v^2} \alpha_1 \alpha_2. \quad (3.7)$$

The calculation goes now in a complete analogy to the Vg case and we arrive at the adapted version of eq. (2.28) into which we plug in the  $T_S^{(F)}$  function

$$\Delta \Gamma_{Vf}^{k_\perp - q} = c_F^V \frac{g^4}{(2\pi)^4} \frac{1}{2\epsilon} \frac{1}{x(1-x)^2} \int d\alpha_1 d\alpha_2 \delta_{1-x-\alpha_1-\alpha_2} \left( \ln(1-x) - 4\theta_{\alpha_2 < \alpha_1} \ln \alpha_1 \right) T_S^{(F)}, \quad (3.8)$$

$$T_S^{(F)} = \frac{\alpha_1}{\alpha_2} x \left( \frac{1}{2} T_{Fc2}^{(0)} + T_{FK}^{(0)} \right) = \frac{1}{2} x(1+x^2) \left( -2 \frac{1}{(1-x)^2} \alpha_1 \alpha_2 + 1 \right). \quad (3.9)$$

Once the  $d\alpha$ -integration is done we obtain the final result for the Vf graph with the cut-off on  $\max k_\perp$

$$\Delta\Gamma_{Vf}^{k_\perp-q} = c_F^V \left( \frac{\alpha}{2\pi} \right)^2 \frac{2}{\epsilon} \frac{1+x^2}{1-x} \left[ -\frac{1}{3} \ln(1-x) + \frac{23}{36} - \frac{2}{3} \ln 2 \right]. \quad (3.10)$$

Let us discuss also the other choices of the cut-offs: the sum of  $k_\perp$ , virtuality and rapidity, labelled as  $\sigma = 0, 1, 2$ , respectively. For this purpose it is enough to repeat the analysis and reuse the formulas for the Vg graph. The formula (2.37) can be directly used to give

$$\begin{aligned} \Delta\Gamma_{Vf}^{\sigma-q} &= c_F^V \frac{g^4}{(2\pi)^4} \frac{1}{2\epsilon} \frac{1}{x(1-x)^2} \int d\alpha_1 d\alpha_2 \delta_{1-x-\alpha_1-\alpha_2} \ln(1-x)^{\sigma-1} T_S^{(F)} \\ &= c_F^V \left( \frac{\alpha_S}{2\pi} \right)^2 \frac{2}{\epsilon} \frac{1+x^2}{1-x} \frac{1}{3} \ln(1-x)^{\sigma-1}. \end{aligned} \quad (3.11)$$

$$\Delta\Gamma_{Vf}^{\Sigma k_\perp-q} = c_F^V \left( \frac{\alpha}{2\pi} \right)^2 \frac{2}{\epsilon} \frac{1+x^2}{1-x} \left[ -\frac{1}{3} \ln(1-x) \right], \quad (3.12)$$

$$\Delta\Gamma_{Vf}^{a-q} = c_F^V \left( \frac{\alpha}{2\pi} \right)^2 \frac{2}{\epsilon} \frac{1+x^2}{1-x} \left[ \frac{1}{3} \ln(1-x) \right]. \quad (3.13)$$

## 4 Virtual diagrams

The shift in virtual corrections due to change of the cut-off can be found in Ref. [9]. The  $\sigma$ -dependence of each diagram is given there. One finds that there is no  $\sigma$ -dependence for the  $C_F^2$ -type graphs and the only ones that do depend on  $\sigma$  are Vg and Vf, see eqs. (4.25) and (4.31) in Ref. [9]. Here we quote the change with respect to the virtuality case:

$$\Delta\Gamma_{virt}^{\sigma-q} = \left( \frac{\alpha}{2\pi} \right)^2 \frac{1}{2\epsilon} C_F \frac{1+x^2}{1-x} \left( \beta_0 - 4C_A (I_0 + \ln(1-x)) \right) \ln^{\sigma-1}(1-x). \quad (4.1)$$

## 5 Combined Vg+Vf real diagrams

Let us combine the Vg and Vf real graphs for the case of  $\max\{k_{1\perp}, k_{2\perp}\}$ . The formulas to be added are (2.29) and (3.10) with  $c_G^V = (1/2)C_F C_A$  and  $c_F^V = C_F T_F$ :

$$\begin{aligned} \Delta\Gamma_{Vf+Vg}^{k_\perp-q} &= C_F \left( \frac{\alpha_S}{2\pi} \right)^2 \frac{2}{\epsilon} \frac{1+x^2}{1-x} \left[ -C_A (I_0 + \ln(1-x)) \ln(1-x) \right. \\ &\quad \left. + C_A \frac{\pi^2}{6} - C_A \frac{1}{16} + \frac{1}{4} \beta_0 \ln(1-x) + \frac{1}{2} \beta_0 \ln 2 - \frac{23}{48} \beta_0 \right], \end{aligned} \quad (5.1)$$

$$\beta_0 = \frac{11}{3} C_A - \frac{4}{3} T_F. \quad (5.2)$$

Anticipating the results of the following sections we can state that this result represents the change of the  $P_{qq}$  kernel due to the real corrections when the evolution variable (cut-off) is changed from the standard  $q^2$  one to  $\max\{k_{1\perp}, k_{2\perp}\}$ . Supplied with the virtual corrections it will give the complete effect.

Let us combine also the  $\sigma$ -type cut-offs for the real Vf+Vg graphs

$$\Delta\Gamma_{Vf+Vg}^{\sigma-q} = C_F \left( \frac{\alpha_S}{2\pi} \right)^2 \frac{1}{2\epsilon} \frac{1+x^2}{1-x} \ln(1-x)^{\sigma-1} \left[ -\beta_0 + 4C_A (I_0 + \ln(1-x)) \right]. \quad (5.3)$$

## 6 Added real and virtual diagrams

We can now add changes of the real and virtual Vf+Vg graphs. For the  $\sigma$ -type cut-offs we observe that the contributions cancel each other and there is no net effect, as expected. The situation is different for the cut-off on  $\max\{k_{1\perp}, k_{2\perp}\}$ , where we find the following shift

$$\Delta\Gamma_{Vf+Vg, R+V}^{k_{\perp}-q} = C_F \left(\frac{\alpha_S}{2\pi}\right)^2 \frac{1}{2\epsilon} \frac{1+x^2}{1-x} \left[ C_A \frac{2\pi^2}{3} - C_A \frac{1}{4} + 2\beta_0 \ln 2 - \frac{23}{12}\beta_0 \right]. \quad (6.1)$$

This result can be translated into the kernel  $P_{qq}$  which is the residue of  $\Gamma$  [5]:

$$\Gamma = \delta_{1-x} + \frac{1}{\epsilon} \left[ \left(\frac{\alpha}{2\pi}\right) P^{(1)} + \frac{1}{2} \left(\frac{\alpha}{2\pi}\right)^2 P^{(2)} + \dots \right], \quad (6.2)$$

$$P_{qq} = \left(\frac{\alpha}{2\pi}\right) P^{(1)} + \left(\frac{\alpha}{2\pi}\right)^2 P^{(2)} + \dots, \quad (6.3)$$

and we obtain the following change of the  $P_{qq}$  kernel

$$\begin{aligned} P_{qq}(\max\{k_{1\perp}, k_{2\perp}\} < Q) - P_{qq}(-q^2 < Q^2) = \\ = C_F \left(\frac{\alpha_S}{2\pi}\right)^2 \frac{1+x^2}{1-x} \left[ C_A \left(\frac{2\pi^2}{3} - \frac{1}{4}\right) + \beta_0 \left(2\ln 2 - \frac{23}{12}\right) \right]. \end{aligned} \quad (6.4)$$

This is the central new result of this paper.

## 7 Br (ladder) graph and counter term

We turn now to the ladder graph and a counter term associated with it, shown in Fig. 1. Both of them have double  $\epsilon$  poles and therefore can be modified once the evolution variable changes. However, we will demonstrate now that their difference remains unchanged.

The contribution  $\Gamma_{Br}$  of the ladder graph is similar to the one given for the Vg graph in eqs. (2.1, 2.2)

$$\Gamma_{Br} = C_F^2 \frac{g^4 x}{(2\pi)^6} \text{PP} \left[ \frac{(2\pi)^{-2\epsilon}}{\mu^{2\epsilon}} \int \frac{d\alpha_2}{2\alpha_2} d^{2+2\epsilon} \vec{k}_{2\perp} \frac{(2\pi)^{-2\epsilon}}{\mu^{2\epsilon}} \int \frac{d\alpha_1}{2\alpha_1} d^{2+2\epsilon} \vec{k}_{1\perp} \delta_{1-x-\alpha_1-\alpha_2} \frac{1}{q^4} \frac{1}{q_1^4} W_{Br} \right]. \quad (7.1)$$

$$W_{Br} = \frac{1}{4qn} \text{Tr} \left( \hat{n} \hat{q} \hat{\gamma}^\mu \hat{q}_1 \hat{\gamma}^\alpha \hat{p} \hat{\gamma}^\beta \hat{q}_1 \hat{\gamma}^\nu \hat{q} \right) d_{\alpha\beta}(k_1) d_{\mu\nu}(k_2). \quad (7.2)$$

$$= \frac{4}{x\alpha_1\alpha_2} \frac{k_{1\perp}^2}{\alpha_1} \left( \frac{k_{1\perp}^2}{\alpha_1} T_1 + \frac{k_{2\perp}^2}{\alpha_2} T_2 + 2\vec{k}_{1\perp} \cdot \vec{k}_{2\perp} T_3 \right), \quad (7.3)$$

$$T_1 = (x^2 + x_1^2 + 1)(1 - x_1)(x_1 - x) + \mathcal{O}(\epsilon), \quad (7.4)$$

$$T_2 = (1 + x_1^2 + \epsilon(1 - x_1)^2)(x^2 + x_1^2 + \epsilon(x_1 - x)^2), \quad (7.5)$$

$$T_3 = x_1(x^2 + x_1^2 + 1) + \mathcal{O}(\epsilon), \quad (7.6)$$

$$q_1^2 = -\frac{k_{1\perp}^2}{\alpha_1} = -\frac{q_{1\perp}^2}{\alpha_1}. \quad (7.7)$$

As before, we will calculate only the difference w.r.t. the result with cut-off on the virtuality,  $-q^2 < Q^2$ . Therefore, the pole coming from  $1/q^2$  integrand is eliminated and we are forced to keep only terms

that generate the  $\epsilon$  pole from the  $dk_{1\perp}^2$  integral. This means that we keep only  $T_2$ , set to zero all other  $\epsilon$ -terms and expand  $dk_{1\perp}^2$ -integral, i.e.

$$\begin{aligned} T_1 = T_3 &= 0, \\ \epsilon &\rightarrow 0 \quad \text{except } k_{1\perp}^{2\epsilon}, \\ \int dk_{1\perp}^2 k_{1\perp}^{-2+2\epsilon} &\rightarrow \frac{1}{\epsilon} \int \delta(k_{1\perp}^2) dk_{1\perp}^2. \end{aligned} \quad (7.8)$$

This way we obtain

$$\Gamma_{Br}^{(q)} = C_F^2 \frac{g^4}{(2\pi)^6} 4\text{PP} \left[ \int_{-q^2 > Q^2} \frac{d\alpha_2}{2\alpha_2^3} d^2 \vec{k}_{2\perp} \int \frac{d\alpha_1}{2\alpha_1} d^{2+2\epsilon} \vec{k}_{1\perp} \delta_{1-x-\alpha_1-\alpha_2} \frac{k_{2\perp}^2}{q^4} \frac{1}{k_{1\perp}^2} T_2(\epsilon=0) \right]. \quad (7.9)$$

The matching counter term  $\Gamma_{Br}^{Ct}$  differs only by the “split” of the trace  $W_{Br}^{Ct}$  and an additional projection operator. The projection operator performs two actions: picks the  $\epsilon$ -poles and sets on-shell the incoming quark ( $q_1$  in our case). These are minor modifications to (7.1, 7.3):

$$\begin{aligned} \Gamma_{Br}^{Ct} &= C_F^2 \frac{g^4}{(2\pi)^6} \text{PP} \left[ \frac{(2\pi)^{-2\epsilon}}{\mu^{2\epsilon}} \int_{-q^2 > Q^2} \frac{d\alpha_2}{2\alpha_2} d^{2+2\epsilon} \vec{k}_{2\perp} \frac{1}{q^4} W_{Br2} \right]_{q_1^2=0} \\ &\times \text{PP} \left( \frac{(2\pi)^{-2\epsilon}}{\mu^{2\epsilon}} \int \frac{d\alpha_1}{2\alpha_1} d^{2+2\epsilon} \vec{k}_{1\perp} \frac{\alpha_1^2}{k_{1\perp}^4} W_{Br1} \delta_{1-x-\alpha_1-\alpha_2} \right), \end{aligned} \quad (7.10)$$

where

$$W_{Br2} = \frac{1}{4qn} \text{Tr} \left( \hat{n} \hat{q} \hat{\gamma}^\mu \hat{q}_1 \hat{\gamma}^\nu \hat{q} \right) d_{\mu\nu}(k_2) \Big|_{q_1^2=0} = -2q^2 \frac{1}{x\alpha_2} (x_1^2 + x^2 + \epsilon(x_1 - x)^2), \quad (7.11)$$

$$W_{Br1} = \frac{1}{4q_1 n} \text{Tr} \left( \hat{n} \hat{q}_1 \hat{\gamma}^\alpha \hat{p} \hat{\gamma}^\beta \hat{q}_1 \right) d_{\alpha\beta}(k_1) = -2q_1^2 \frac{1}{x_1 \alpha_1} (1 + x_1^2 + \epsilon(1 - x_1)^2), \quad (7.12)$$

and thanks to the condition  $q_1^2 = 0$ :

$$q_1^2 = -\frac{k_{1\perp}^2}{\alpha_1}, \quad q^2 \Big|_{q_1^2=0} = -x \left( \frac{k_{1\perp}^2}{\alpha_1} + \frac{k_{2\perp}^2}{\alpha_2} \right) - k_{\perp}^2 \Big|_{k_{1\perp}^2=0} = -\frac{x_1 k_{2\perp}^2}{\alpha_2}. \quad (7.13)$$

We obtain

$$\Gamma_{Br}^{Ct} = C_F^2 \frac{g^4}{(2\pi)^6} 4\text{PP} \left[ \int_{-q^2 > Q^2} \frac{d\alpha_2}{2\alpha_2^3} d^2 \vec{k}_{2\perp} \frac{k_{2\perp}^2}{q^4} \Big|_{q_1^2=0} \int \frac{d\alpha_1}{2\alpha_1} d^{2+2\epsilon} \vec{k}_{1\perp} \frac{1}{k_{1\perp}^2} \delta_{1-x-\alpha_1-\alpha_2} T_2(\epsilon=0) \right]. \quad (7.14)$$

It is easy to verify now that these two quantities,  $\Gamma_{Br}$  and  $\Gamma_{Br}^{Ct}$ , are identical under the conditions (7.8) and the net change of the kernel is zero.

In Appendix A we evaluate the change of the ladder graph alone caused by the change of cut-off. This quantity is of interest for example in the construction of Monte Carlo algorithms.

## 8 Conclusions

In this paper we have discussed the change of the DGLAP kernel  $P_{qq}$  due to the change of the evolution variable. We have demonstrated that at the NLO level majority of the choices of the evolution variables

lead to the same kernel, but there are ones, like maximal transverse momentum, that correspond to modified kernel. We have shown the mechanism responsible for the change and we have formulated a simple rule to identify classes of variables that leave the kernel unchanged at the NLO level.

There is an important open question related to our analysis: is the kernel dependence specific to the CFP method and specifically to the presence of the geometrical cut-off  $\delta$ ? If all the singularities, including the “spurious” ones, were regulated by the dimensional regularization, the structure of the  $\epsilon$  poles would be reached, more graphs would have higher-order poles in  $\epsilon$  and would contribute to the modification of the kernel. This would, however, be a surprising result showing that the choice of the seemingly dummy technical regulator has a physical consequences. The same question holds for the modification of the original PV prescription of [5] to the NPV one used in this note.

## Acknowledgments

This work is partly supported by the Polish National Science Center grant DEC-2011/03/B/ST2/02632 and the Polish National Science Centre grant UMO-2012/04/M/ST2/00240.

## A Change of ladder graph with cut-off

In the appendix we calculate change of the  $\Gamma_{Br}$  for various cut-offs as it can be useful in constructing MC algorithms. Let us continue with eq. (7.1) and let us implement the conditions (7.8):

$$\int d^{2+2\epsilon} \vec{k}_{1\perp} \frac{1}{k_{1\perp}^2} = \int \frac{1}{2} \frac{dk_{1\perp}^2}{k_{1\perp}^2} k_{1\perp}^{2\epsilon} d\Omega_{1+\epsilon}^{(k_{1\perp})} \rightarrow \int \frac{1}{2} dk_{1\perp}^2 \frac{1}{\epsilon} \delta(k_{1\perp}^2) d\Omega_1^{(k_{1\perp})} = 2\pi \frac{1}{2\epsilon} \quad (\text{A.1})$$

$$\int_L^U d^{2+2\epsilon} \vec{k}_{2\perp} \frac{1}{k_{2\perp}^2} \rightarrow \int_L^U \frac{1}{2} dk_{2\perp}^2 k_{2\perp}^{-2} d\Omega_1^{(k_{2\perp})} = \pi \ln \frac{U}{L}. \quad (\text{A.2})$$

The lower limit on integral  $d^{2+2\epsilon} \vec{k}_{2\perp}$  follows from the fact that we compute the difference w.r.t. the virtuality-based formula. This leads to the condition

$$Q^2 < -q^2 = \frac{x_1 k_{2\perp}^2}{\alpha_2} \rightarrow k_{2\perp}^2 > Q^2 \frac{\alpha_2}{x_1}. \quad (\text{A.3})$$

The upper limit depends on the chosen evolution variable. We will examine a few cases. The cut-offs and their simplified version once the condition (A.1), i.e.  $k_{1\perp} = 0$ , is applied are as follows:

$$\left. \begin{array}{l} (A): \max\{k_{1\perp}, k_{2\perp}\} \\ (B): k_{1\perp} + k_{2\perp} \\ (C): \max\left\{\frac{k_{1\perp}}{\alpha_1}, \frac{k_{2\perp}}{\alpha_2}\right\} \\ (D): \frac{|\vec{k}_{1\perp} + \vec{k}_{2\perp}|}{\alpha_1 + \alpha_2} \end{array} \right\} \xrightarrow{k_{1\perp}=0} \left\{ \begin{array}{l} (A): k_{2\perp} < Q \\ (B): k_{2\perp} < Q \\ (C): k_{2\perp} < \alpha_2 Q \\ (D): k_{2\perp} < (1-x)Q \end{array} \right. \quad (\text{A.4})$$

Eq. (7.1) transforms now into

$$\Delta \Gamma_{Br}^{U-q^2} = C_F^2 \left( \frac{\alpha}{2\pi} \right)^2 \left[ \int \frac{d\alpha_2}{\alpha_2} \ln \frac{U}{L} \int \frac{d\alpha_1}{\alpha_1} \frac{1}{2\epsilon} \delta_{1-x-\alpha_1-\alpha_2} \frac{1}{x_1^2} (1+x_1^2)(x^2+x_1^2) \right]. \quad (\text{A.5})$$

Let us continue with each case separately.

**Cases (A) and (B):**  $\max\{k_{1\perp}, k_{2\perp}\}$  **and**  $k_{1\perp} + k_{2\perp}$

$$\Gamma_{Br}^{k_{\perp}-q^2} = C_F^2 \left( \frac{\alpha}{2\pi} \right)^2 \frac{1}{2\epsilon} \int_0^{1-x} \frac{d\alpha_1}{\alpha_1 \alpha_2} \frac{1}{x_1^2} (1+x_1^2)(x^2+x_1^2) \ln \frac{x_1}{\alpha_2} \quad (\text{A.6})$$

$$= C_F^2 \left( \frac{\alpha}{2\pi} \right)^2 \frac{1}{2\epsilon} \frac{1}{1-x} \int_0^{1-x} d\alpha_1 (U_0 + U_l + U_u),$$

$$U_0 = \left( \frac{1}{1-x_1} + \frac{1}{x_1-x} \right) \frac{1}{x_1^2} (1+x_1^2)(x^2+x_1^2) \ln \frac{x_1}{x_1-x} - U_l - U_u, \quad (\text{A.7})$$

$$U_l = \frac{1}{1-x_1} 2(1+x^2) \ln \frac{1}{1-x}, \quad (\text{A.8})$$

$$U_u = \frac{1}{x_1-x} 2(1+x^2) \ln \frac{x}{x_1-x}, \quad (\text{A.9})$$

where we have subtracted and added the singular integrals of the  $I_{0,1}$  type. Direct integration gives

$$\begin{aligned} \int_0^{1-x} d\alpha_1 U_0 = & - (1-x)^2 + (1+x^2) \ln^2 x + (1+3x^2) \frac{\pi^2}{6} + 2(1-x)^2 \ln(1-x) \\ & - (x^2-1) \text{Li}_2(x) + x(1-x) \ln x \end{aligned} \quad (\text{A.10})$$

$$\int_0^{1-x} d\alpha_1 U_l = 2(1+x^2)(I_0 + \ln(1-x)) \ln \frac{1}{1-x} \quad (\text{A.11})$$

$$\begin{aligned} \int_0^{1-x} d\alpha_1 U_u = & 2(1+x^2)(I_0 + \ln(1-x)) \ln x - 2(1+x^2) \left( I_1 + \frac{1}{2} \ln^2(1-x) \right) \\ = & 2(1+x^2) \left( -I_1^{(1-x)} + I_0^{(1-x)} \ln \frac{x}{1-x} \right), \end{aligned} \quad (\text{A.12})$$

where

$$\begin{aligned} I_0^{(1-x)} &= I_0 + \ln(1-x), \\ I_1^{(1-x)} &= I_1 - I_0 \ln(1-x) + \frac{1}{2} \ln^2(1-x). \end{aligned} \quad (\text{A.13})$$

Hence

$$\begin{aligned} \Gamma_{Br}^{k_{\perp}-q^2} = & C_F^2 \left( \frac{\alpha}{2\pi} \right)^2 \frac{1}{2\epsilon} \left[ -(1-x) - (1+x) \frac{\pi^2}{6} + 2(1-x) \ln(1-x) + (1+x) \text{Li}_2(x) \right. \\ & \left. + x \ln x + 2 \frac{1+x^2}{1-x} \left( -I_1^{(1-x)} + I_0^{(1-x)} \ln \frac{x}{(1-x)^2} + \frac{1}{2} \ln^2 x + \frac{\pi^2}{6} \right) \right]. \end{aligned} \quad (\text{A.14})$$

**Case (C):**  $\max\left\{\frac{k_{1\perp}}{\alpha_1}, \frac{k_{2\perp}}{\alpha_2}\right\}$

$$\Gamma_{Br}^{k_{\perp}/a-q^2} = C_F^2 \left(\frac{\alpha}{2\pi}\right)^2 \frac{1}{2\epsilon} \int_0^{1-x} \frac{d\alpha_1}{\alpha_1 \alpha_2} \frac{1}{x_1^2} (1+x_1^2)(x^2+x_1^2) \ln(x_1 \alpha_2) \quad (\text{A.15})$$

$$= C_F^2 \left(\frac{\alpha}{2\pi}\right)^2 \frac{1}{2\epsilon} \left[ 1-x + (1+x) \ln^2 x + (1+x) \frac{\pi^2}{6} - 2(1-x) \ln(1-x) - (2-x) \ln x \right. \\ \left. - (1+x) \text{Li}_2(x) + 2 \frac{1+x^2}{1-x} \left( I_1^{(1-x)} + I_0^{(1-x)} \ln(x(1-x)^2) - \frac{\pi^2}{6} + \frac{1}{2} \ln^2 x \right) \right]. \quad (\text{A.16})$$

**Case (D):**  $|\vec{k}_{1\perp} + \vec{k}_{2\perp}|/(\alpha_1 + \alpha_2)$

$$\Gamma_{Br}^{k_{\perp}/(1-x)-q^2} = C_F^2 \left(\frac{\alpha}{2\pi}\right)^2 \frac{1}{2\epsilon} \int_0^{1-x} \frac{d\alpha_1}{\alpha_1 \alpha_2} \frac{1}{x_1^2} (1+x_1^2)(x^2+x_1^2) \ln \frac{x_1(1-x)}{\alpha_2} \\ = C_F^2 \left(\frac{\alpha}{2\pi}\right)^2 \frac{1}{2\epsilon} \left[ -(1-x) - (1+x) \text{Li}_2(1-x) + x \ln x \right. \\ \left. 2 \frac{1+x^2}{1-x} \left( -I_1^{(1-x)} + I_0^{(1-x)} \ln x + \frac{\pi^2}{6} + \frac{1}{2} \ln^2 x \right) \right]. \quad (\text{A.17})$$

## References

- [1] M. Bengtsson, T. Sjostrand, A Comparative Study of Coherent and Noncoherent Parton Shower Evolution, Nucl. Phys. B289 (1987) 810–846. [doi:10.1016/0550-3213\(87\)90407-X](https://doi.org/10.1016/0550-3213(87)90407-X).
- [2] T. Sjostrand, A model for initial state parton showers, Phys. Lett. B157 (1985) 321.
- [3] T. Sjostrand, P. Z. Skands, Transverse-momentum-ordered showers and interleaved multiple interactions, Eur. Phys. J. C39 (2005) 129–154. [arXiv:hep-ph/0408302](https://arxiv.org/abs/hep-ph/0408302), [doi:10.1140/epjc/s2004-02084-y](https://doi.org/10.1140/epjc/s2004-02084-y).
- [4] M. Bahr, et al., Herwig++ Physics and Manual, Eur. Phys. J. C58 (2008) 639–707. [arXiv:0803.0883](https://arxiv.org/abs/0803.0883), [doi:10.1140/epjc/s10052-008-0798-9](https://doi.org/10.1140/epjc/s10052-008-0798-9).
- [5] G. Curci, W. Furmanski, R. Petronzio, Evolution of parton densities beyond leading order: the non-singlet case, Nucl. Phys. B175 (1980) 27.
- [6] R. K. Ellis, H. Georgi, M. Machacek, H. D. Politzer, G. G. Ross, Factorization and the Parton Model in QCD, Phys. Lett. B78 (1978) 281.
- [7] G. Heinrich, [Improved techniques to calculate two-loop anomalous dimensions in QCD](https://arxiv.org/abs/1303.0549), Ph.D. thesis, Swiss Federal Institute of Technology, Zurich (1998). URL <http://dx.doi.org/10.3929/ethz-a-001935934>
- [8] S. Jadach, A. Kusina, M. Skrzypek, M. Slawinska, Two real parton contributions to non-singlet kernels for exclusive QCD DGLAP evolution, JHEP 08 (2011) 012. [arXiv:1102.5083](https://arxiv.org/abs/1102.5083), [doi:10.1007/JHEP08\(2011\)012](https://doi.org/10.1007/JHEP08(2011)012).
- [9] O. Gituliar, Higher-Order Corrections in QCD Evolution Equations and Tools for Their Calculation, Ph.D. thesis, Institute of Nuclear Physics, Cracow (2014), [arXiv:1403.6897](https://arxiv.org/abs/1403.6897).
- [10] O. Gituliar, S. Jadach, A. Kusina, M. Skrzypek, On regularizing the infrared singularities in QCD NLO splitting functions with the new Principal Value prescription, Phys.Lett. B732 (2014) 218–222. [arXiv:1401.5087](https://arxiv.org/abs/1401.5087), [doi:10.1016/j.physletb.2014.03.045](https://doi.org/10.1016/j.physletb.2014.03.045).



- [11] M. Skrzypek, O. Gituliar, S. Jadach, A. Kusina, The new PV prescription for IR singularities of NLO splitting functions, PoS LL2014 (2014) 059. [arXiv:1407.6261](#).